Electronic Supplementary Material (ESI) for Journal of Materials Chemistry A.
This journal is © The Royal Society of Chemistry 2018

Journal of
Materials Chemistry A
ELECTRONIC SUPPLEMENTARY INFORMATION (ESI†)

Rational design of forest-like nickel sulfide hierarchical architectures with ultrahigh areal capacity as a binder-free cathode material for hybrid supercapacitors†

G. Seeta Rama Raju,[a] E. Pavitra,[b] Goli Nagaraju,[c] S. Chandra Sekhar,[d] Seyed Majid Ghoreishian,[b] Cheol Hwan Kwak,[b] Jae Su Yu,*[d] Yun Suk Huh,*[b] and Young-Kyu Han,*[a]

[a]*Department of Energy and Materials Engineering, Dongguk University–Seoul, Seoul 04620, Republic of Korea*

[b]*Department of Biological Engineering, Biohybrid Systems Research Center (BSRC), Inha University, Incheon, 22212, Republic of Korea*

[c]*Department of Chemical Engineering, College of Engineering, Kyung Hee University, 1732 Deogyeong-daero, Gihung-gu, Yongin-si, Gyeonggi-do 17104, Republic of Korea*

[d]*Department of Electronic Engineering, Institute for Wearable Convergence Electronics, Kyung Hee University, 1732 Deogyeong-daero, Gihung-gu, Yongin-si, Gyeonggi-do 17104, Republic of Korea*

Corresponding Authors

**Email: jsyu@khu.ac.kr (J. S. Yu)*

**Email: yunsuk.huh@inha.ac.kr (Y. S. Huh)*

**Email: ykenergy@dongguk.edu (Y.-K. Han)*

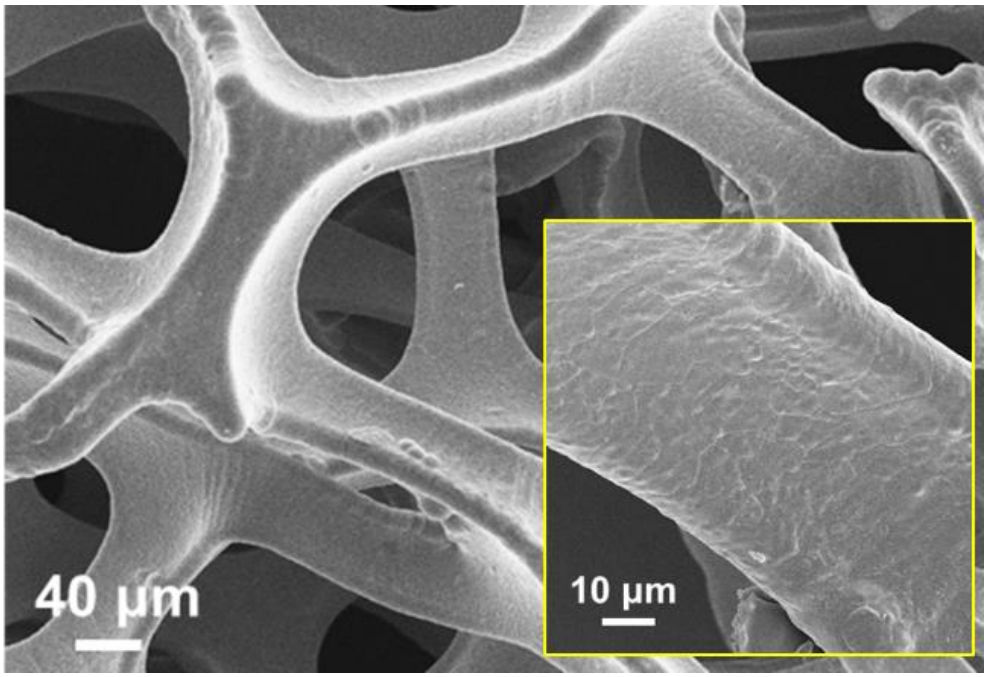

Fig. S1 FE-SEM images of pristine Ni foam, showing its porous conductive frames with smooth surface.

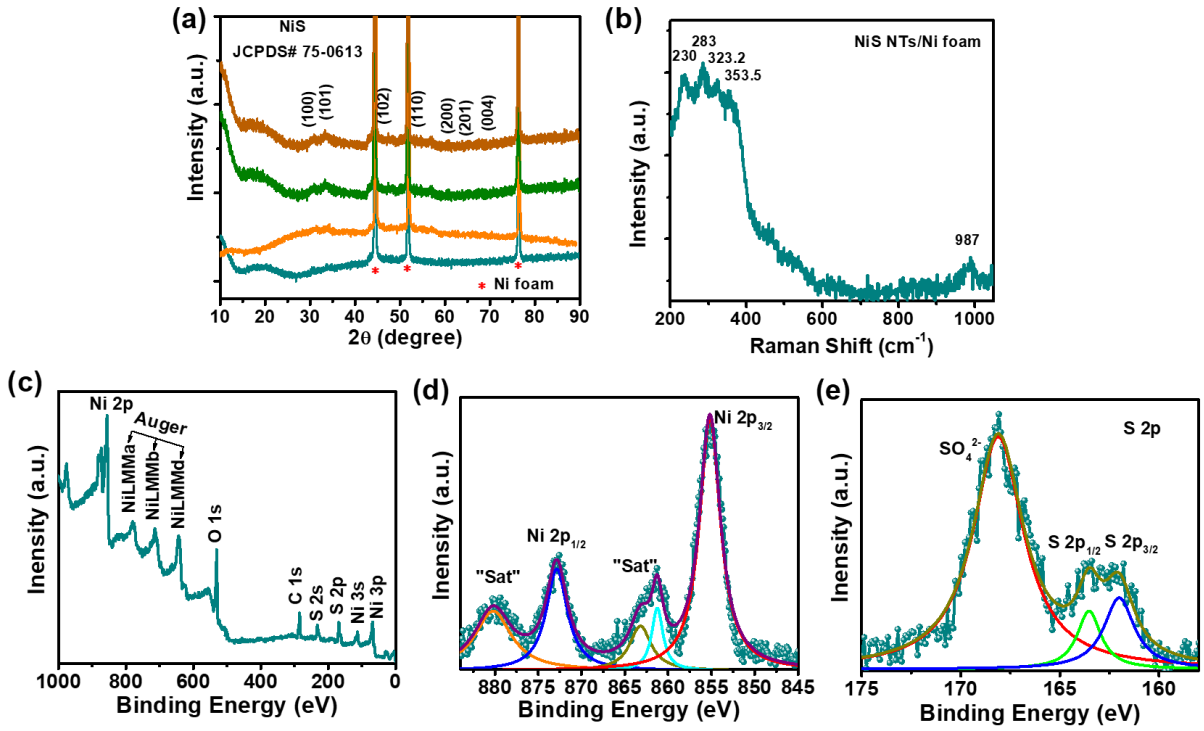

Fig. S2 (a) XRD patterns of NiS-based samples synthesized under different time intervals [i) 1 h, ii) 2 h, iii) 3 h and iv) 5 h], (b) HR-Raman, and (c–e) XPS survey scan spectrum, high-resolution Ni 2p and S 2p XPS spectra, respectively, of forest-like NiS NTs/Ni foam sample under the optimal growth condition of 85 °C for 3 h.

Section 1: Structural, morphological and electrochemical properties of NiS on Ni foam without using the nickel salt in the growth solution:

Fig. S3a-c shows the low and high-magnification FE-SEM images of the nanostructured NiS on Ni foam, which was developed without Ni salt ($Ni(NO_3)_2 \cdot 6H_2O$ source) in the growth solution. Interestingly, NiS nanoparticles were observed on the Ni foam with a mass loading of 0.9 mg/cm^2 at the reaction temperature of 85 ºC for 3 h. This indicates that, forest-like NiS NTs on Ni foam were not formed without the addition of nickel salt in the growth solution. The structural and electrochemical properties of the corresponding sample was also examined. From the EDX (taken from FE-SEM equipment) and XRD results (Fig. S3d-e), it is evident that the prepared sample (without the addition of nickel salt) composed of Ni and S elements has pure NiS phase without any impurities. The XRD pattern of NiS/Ni foam showed low intense peaks, which may be due to the less amount material deposited on the spectrum. Furthermore, when tested the electrochemical properties in 1 M KOH solution, the NiS nanoparticles coated Ni foam exhibited a battery-type redox behavior, confirmed from the CV and GCD curves (Fig. S3f-g and Fig. S4a-b), which is similar to the forest-like NiS NTs electrode behavior. However, NiS nanoparticles coated Ni foam sample exhibited relatively low electrochemical performance compared to the forest-like NiS NTs/Ni foam electrode, as shown in Fig. S4a-b. The obtained results indicate that the inclusion of nickel salt in growth solution help to increase the nucleation and precipitation rate to form the hierarchically designed forest-like NiS NTs for the enhancement of energy storage performance.

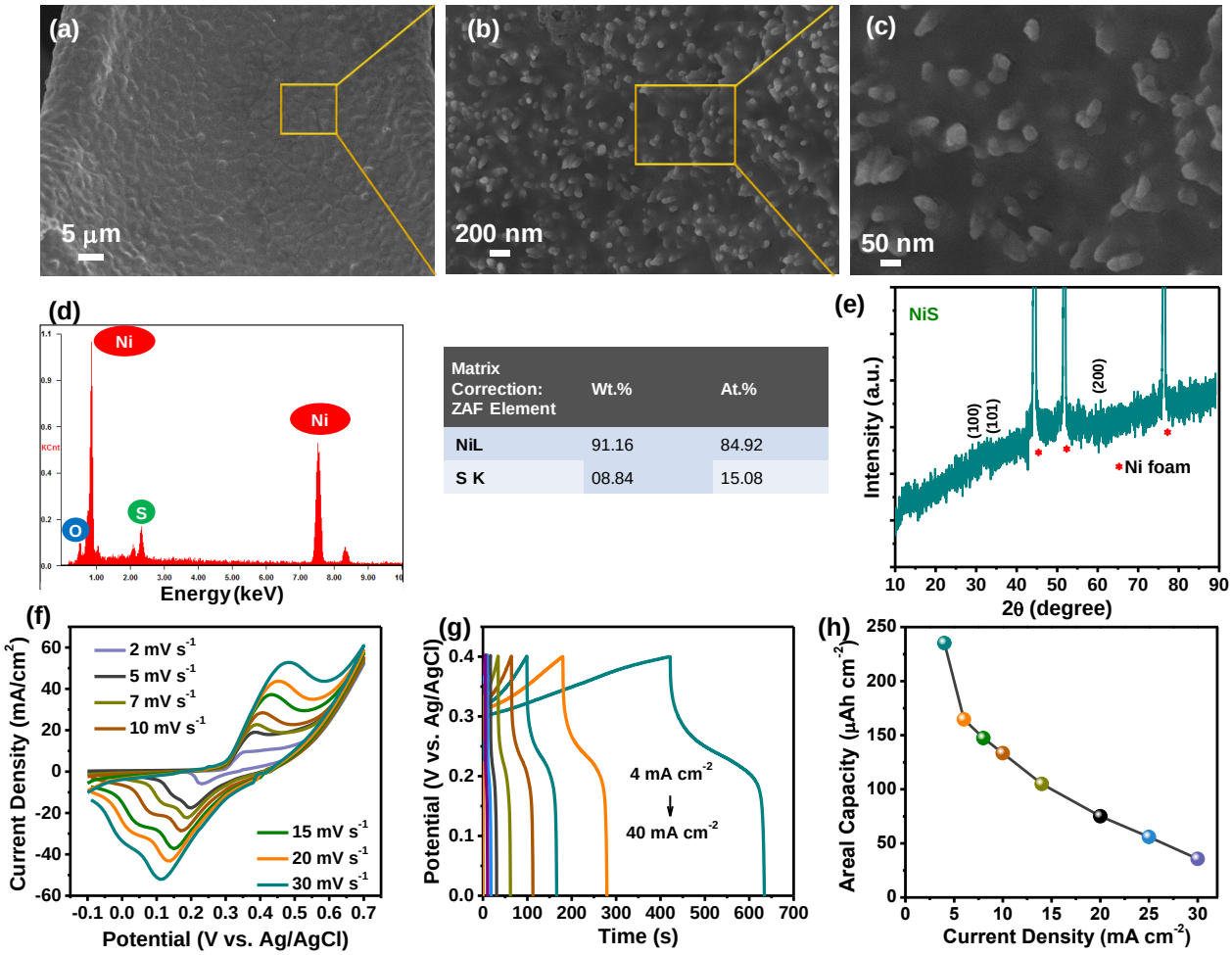

Fig. S3. Physical and electrochemical properties of NiS nanoparticles coated Ni foam, which was prepared without addition of nickel salt in the growth solution. (a-c) low- and high-magnification FE-SEM images of NiS nanoparticles, (d-e) EDX and XRD pattern of the same sample. (f-h) CV curves, GCD curves and calculated areal capacity values of NiS nanoparticles coated Ni foam electrode, respectively.

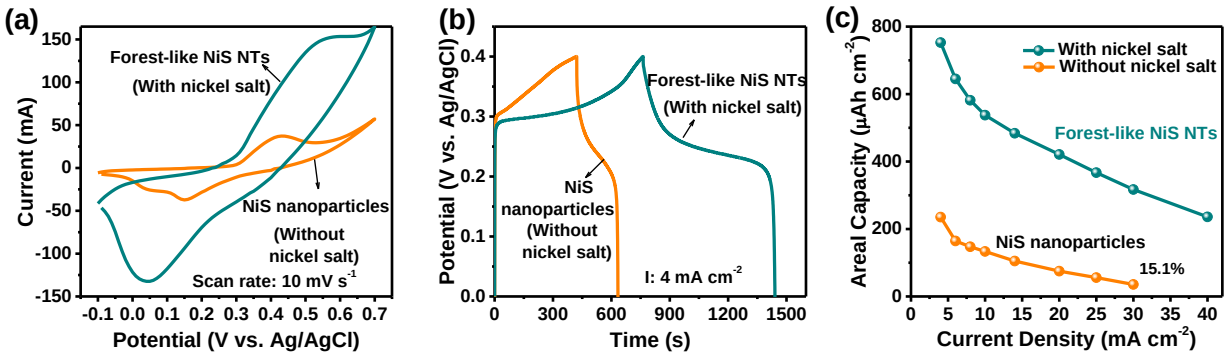

Fig. **S4**. Comparative electrochemical properties of NiS nanoparticles and forest-like NiS NTs, which were prepared with and without inclusion of nickel salt in the growth solution. (a) CV curves (b) GCD curves and calculated capacity values of the both samples. This results indicate that the sample prepared with an inclusion of nickel salt (i.e., forest-like NiS NTs) ensued superior capacity values than the sample synthesized without addition of nickel salt in the growth solution.

Section 2: Effect of growth temperature on the morphological and electrochemical properties of NiS nanostructures on Ni foam: The effect of growth time on the structural and electrochemical properties of NiS on Ni foam were carried out under different temperatures of 50-115 °C with a constant growth time of 3 h. At the low growth temperature (50 °C), as shown in FE-SEM images of Fig. S5a, NiS with nanosheet like morphology was started to grew on Ni foam substrate. This means that the growth temperature is not enough to form the vertically aligned forest-like nanoarchitectures. With increasing the growth temperature to 85 °C, the forest-like NiS NTs were uniformly distributed on Ni foam due to the increased nucleation and growth rate of the added reactants (see FE-SEM images of Fig. 2). Further increasing the growth temperature to 115 °C (Fig. S5b), NiS nanostructures were densely integrated on Ni foam in the form of lumps with high mass loading. Also, several cracks were observed due to the extreme growth rate and

precipitation of added reactants. This kind of cracks may not useful for improving the capacity and rate capability of the prepared samples.

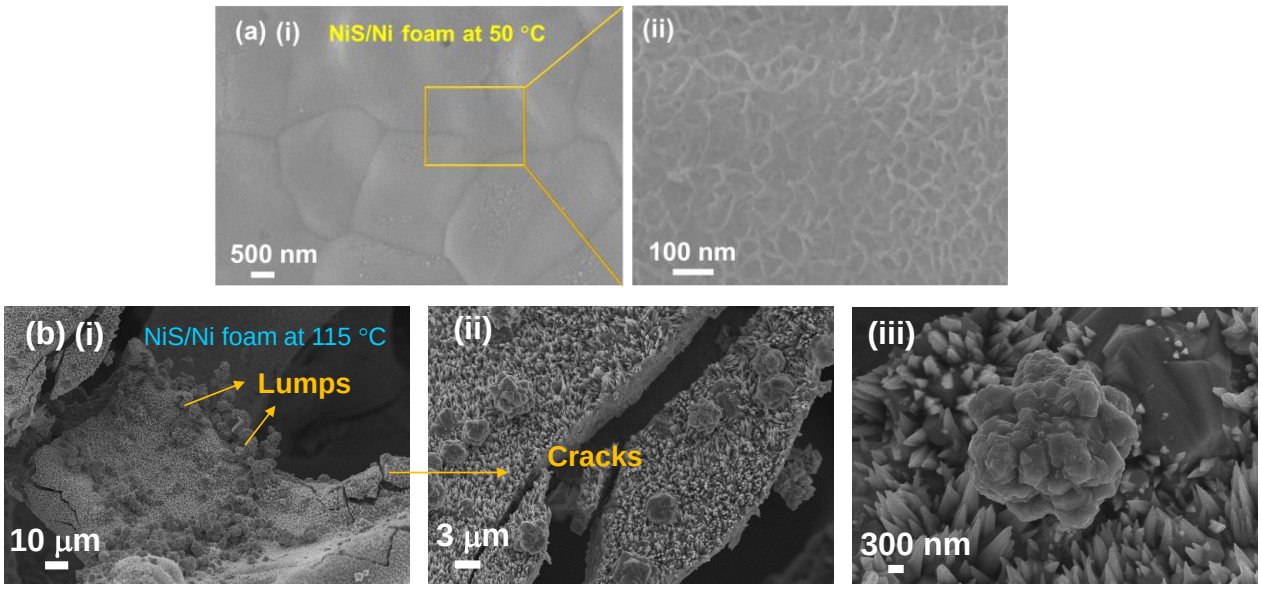

Fig. S5. FE SEM images of NiS nanostructures prepared at the growth temperatures of (a) 50 °C and (b) 115 °C.

The electrochemical properties of the prepared samples under different temperatures were included in Fig. S6. The comparative CV curves (measured at a scan rate of 10 mV/s), shown in Fig. S6a displayed the dynamic redox peaks, indicating the battery-type mechanism of NiS-based samples. Compared to other samples, the forest-like NiS NTs synthesized at 85 °C exhibited higher redox current and large enclosed CV area, revealing the high capacity contribution of the material. To estimate the capacity of the prepared samples, the GCD curves (Fig. S6b) also measured as a function of synthesis temperature. As shown in the comparative GCD curves (measured at a constant current density of 4 mA/cm^2), the sample synthesized at high temperature (115 °C) demonstrated uneven charge-discharge times, where the material showed high charge time and small discharge time, which indicates the low columbic efficiency of the prepared sample and this could be due to the surface cracks and over mass loading of the material. On the other hand, as

shown in discharge curves of the prepared electrodes, the NiS synthesized at 85 °C demonstrated high discharge time compared to the other growth temperature samples. The calculated discharge capacities of these samples were plotted in Fig. S6c, which showed the areal capacities of 287.37, 752.71 and 386.88 $\mu Ah/cm^2$ for the NiS nanostructures prepared at various growth temperatures of 50, 85, and 115 °C, respectively. Thus, we have chosen 85 °C and 3 h were the optimal growth conditions in the development of forest-like NiS NTs as a high capacity cathode material for the hybrid supercapacitors. The overall electrochemical properties, including CV at various scan rates, GCD at different current densities and calculated capacity plots, of NiS samples developed at 50 and 115 °C, were presented in Fig. S7.

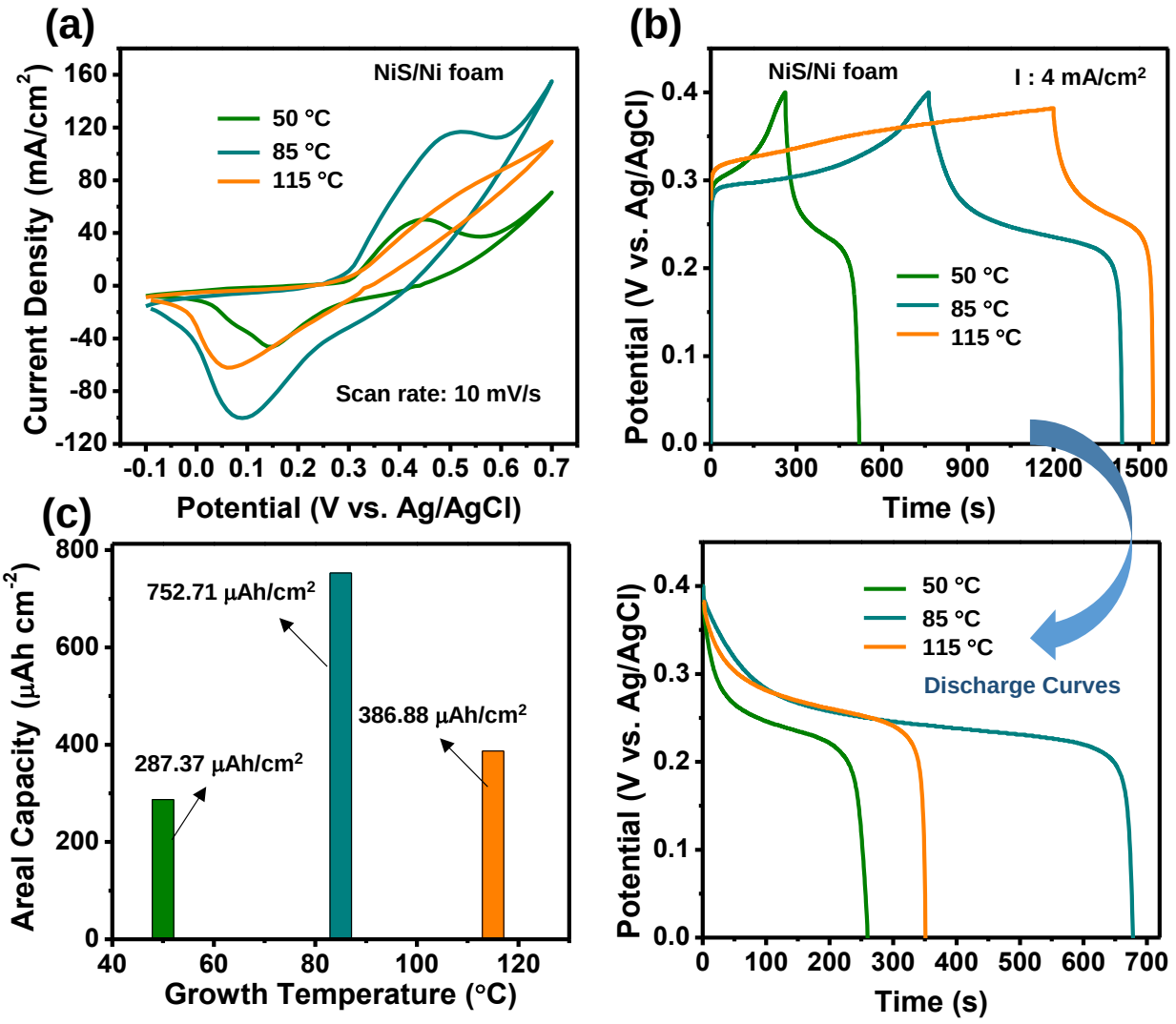

Fig. S6. Comparative electrochemical properties of NiS nanostructures prepared under various growth temperatures.

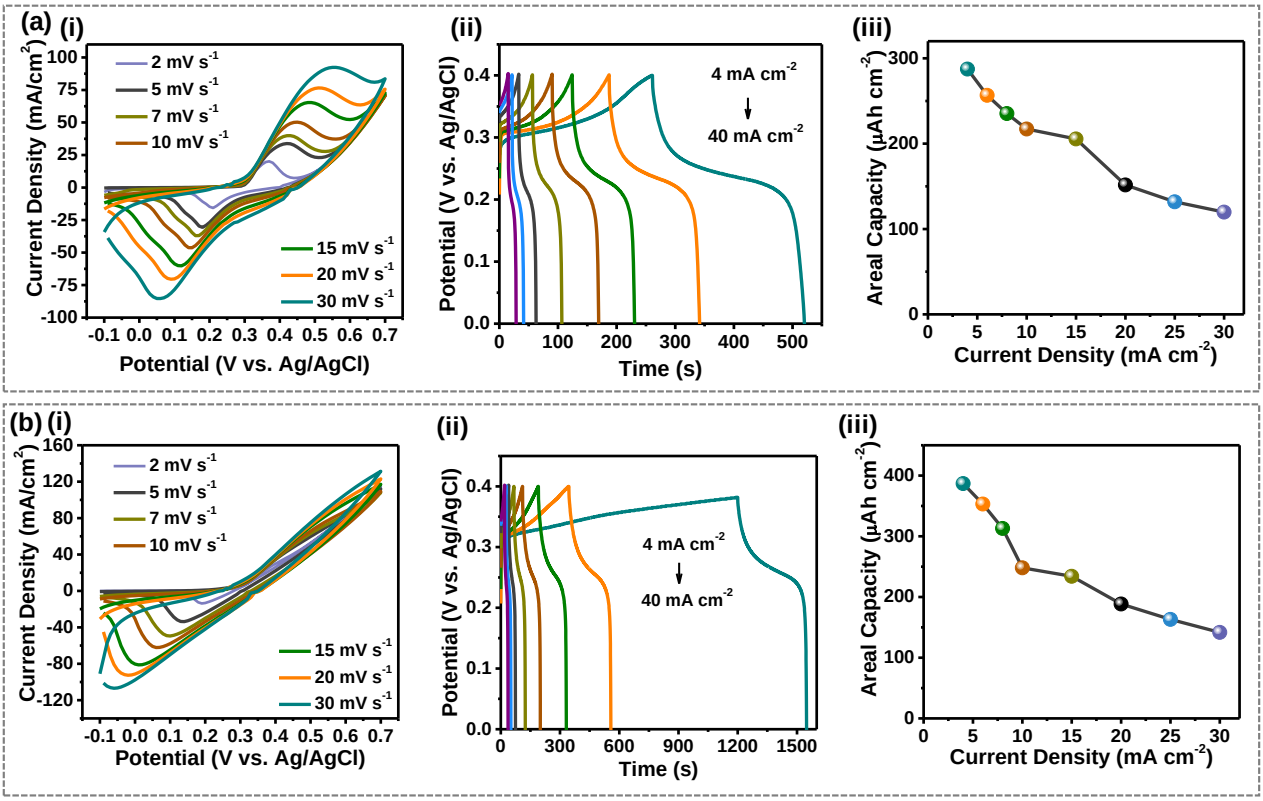

Fig. S7. CV curves, GCD curves and calculated areal capacity values of the NiS-based samples synthesized at various growth temperatures of (a) 50 °C and (b) 115 °C, respectively.

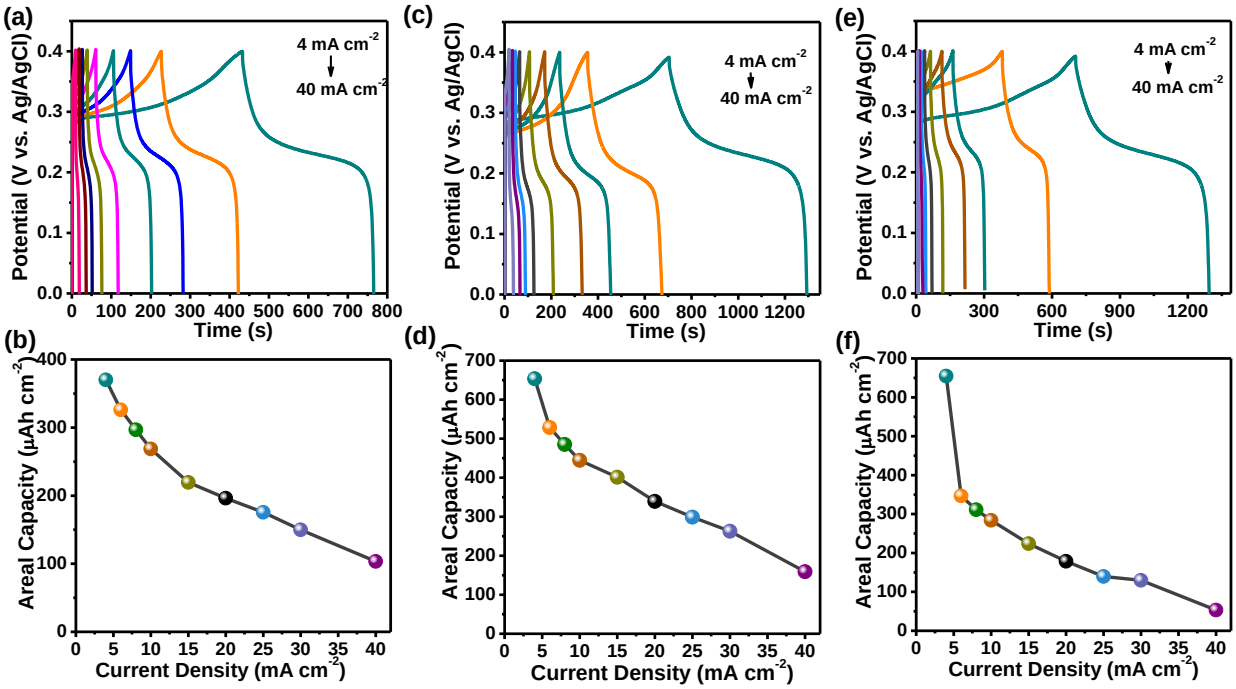

Fig. S8. Electrochemical performance of NiS-based sampled deposited under different growth times of (a-b) 1 h, (c-d) 2 h and (e-f) 5 h, respectively with a constant growth temperature of 85 °C.

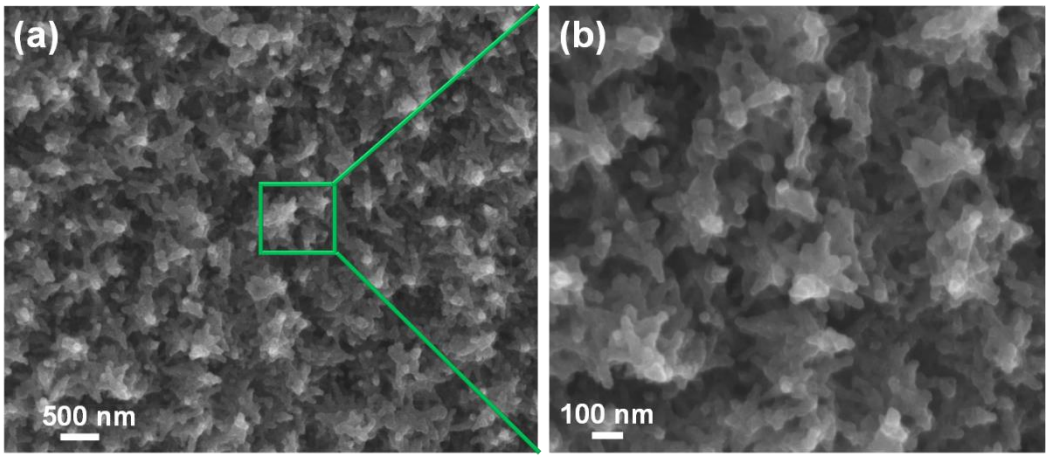

Fig. S9 FE-SEM images of the forest-like NiS NTs/Ni foam after cycling test in three-electrode system.

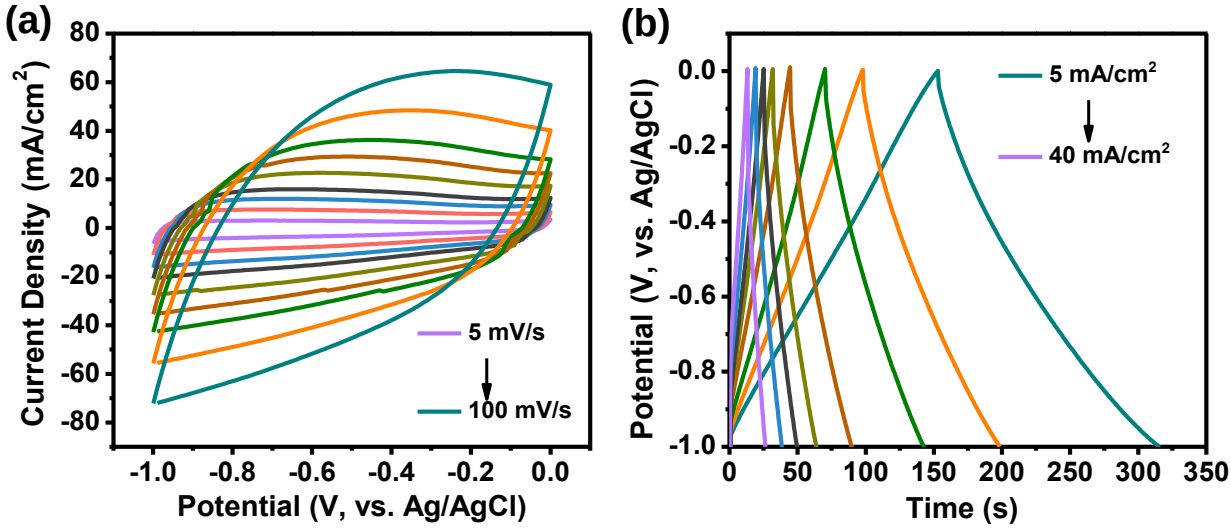

Fig. S10 (a) CV (b) GCD curves of PAC/Ni foam electrode in 1 M KOH solution.

Table S1. Comparative electrochemical properties of previously reported metal sulfide/selenide based nanostructures with forest-like NiS NTs/Ni foam electrode.

Electroactive material	Current collector	Electrolyte	Test condition (mA/cm^2)	Area (cm^2)	Areal capacity ($\mu Ah/cm^2$)	Ref.
Ni_3S_2 nanoparticles	Carbon fiber paper	2 M KOH	2	1	119.44	S1
NiSe microspheres	Ni foam	2 M KOH	3	0.6	1250	S2
Ni_3S_2 nanosheets	Ni foam	1 M KOH	1	1	154.16	S3
NiS box-in-box	Ni foam	3 M KOH	1	1	63.8	S4
Ni_3S_2@MWCNTs composite	Ni foam	2 M KOH	1.2	1	191.6	S5
NiSe nanowires	Ni foam	2 M KOH	5	1	700.1	S6
NiS nanoframes	Ni foam	6 M KOH	1	1	279.16	S7
NiS hollow spheres	Ni foam	2 M KOH	4.08	1	147.3	S8
CoS hollow tubes	Ni foam	6 M KOH	5	1.13	472.2	S9
CuS nanonedles@CNT	Ni foam	2 M KOH	2.9	1	40.7	S10
NiS nanostructures	Graphene-Cotton	6 M KOH	0.5	1	172.1	S11
Forest-like NiS NTs	Ni foam	1 M KOH	4	1	752.71	This work

References.

S1. W. Yu, W. Lin, X. Shao, Z. Hu, R. Li and D. Yuan, J. Power Sources, 2014, **272**, 137-143.

S2. K. Guo, F. Yang, S. Cui, W. Chen and L. Mi, RSC Adv., 2016, **6**, 46523-46530.

S3. S.-W. Chou and J.-Y. Lin, J. Electrochem. Soc., 2013, **160**, D178-D182.

S4. X.-Y. Yu, L. Yu, L. Shen, X. Song, H. Chen and X. W. Lou, Adv. Funct. Mater., 2014, **24**, 7440-7446.

S5. C.-S. Dai, P.-Y. Chien, J.-Y. Lin, S.-W. Chou, W.-K. Wu, P.-H. Li, K.-Y. Wu and T.-W. Lin, Acs. Appl. Mater. Interfaces., 2013, **5**, 12168-12174.

S6. C. Tang, Z. Pu, Q. Liu, A. M. Asiri, X. Sun, Y. Luo and Y. He, ChemElectroChem, 2015, **2**, 1903-1907.

S7. X.-Y. Yu, L. Yu, H. B. Wu and X. W. Lou, Angew. Chem. Int. Ed., 2015, **54**, 5331-5335.

S8. B. T. Zhu, Z. Wang, S. Ding, J. S. Chen and X. W. Lou, RSC Adv., 2011, **1**, 397-400.

S9. H. Wan, X. Ji, J. Jiang, J. Yu, L. Miao, L. Zhang, S. Bie, H. Chen and Y. Ruan, J. Power Sources, 2013, **243**, 396-402.

S10. T. Zhu, B. Xia, L. Zhou and X. Wen Lou, J. Mater. Chem., 2012, **22**, 7851-7855.

S11. Y. Li, K. Ye, K. Cheng, J. Yin, D. Cao and G. Wang, J. Power Sources, 2015, **274**, 943-950.